International Journal of Communication Networks and Information Security
2024, 16(s1)
ISSN: 2073-607X,2076-0930
https://ijcnis.org/

Research Article

Enhanced Medical Image Reconstruction Using Deep Learning Classification: A High-Resolution, Noise-Resilient Approach

Shivganga Patil [1] and Lakshmi Patil [2]

[1]Research Scholar , Department of Electronics and Communication Engineering , Sharnbasva UniversityKalaburagi, India
[2]Research Supervisor , Department of Electronics and Communication Engineering , Sharnbasva University Kalaburagi, India
[1]shivgangabp@yahoo.co.in ; [2]patillakshmi192@gmail.com

ARTICLE INFO

Received: 1 Aug 2024
Accepted: 5 Sep 2024

ABSTRACT

This study introduces a novel deep learning classification (DLC) method for reconstructing high-resolution medical images, showcasing its superiority over traditional techniques such as zero-filled (ZF) and compressed sensing (CS), as well as deep learning regression methods with L1 (DLR-L1) and L2 (DLR-L2) loss functions. Unlike conventional methods, DLC generates a probability distribution for each pixel, allowing for the approximation of continuous pixel values, which effectively reduces quantization errors and preserves fine image details. To address the computational challenges of high bit-depth imaging, a divide-and-conquer strategy was implemented, enabling the DLC network to handle 16-bit images without a significant increase in network parameters. The DLC method's performance was compared to ZF, CS, DLR-L1, and DLR-L2 across scenarios with high acceleration factors, low signal-to-noise ratios (SNR), and high bit-depths. The results demonstrated that DLC consistently produced images with superior resolution, sharper edges, and better preservation of low-contrast features. Quantitative metrics, including structural similarity index (SSI), peak signal-to-noise ratio (PSNR), relative error, and mean squared error (MSE), further validated the DLC method's superiority, particularly in noisy environments. These findings highlight the potential of DLC as a powerful tool in medical imaging, offering significant improvements in image quality and diagnostic accuracy across various applications.

Keywords: Deep learning classification; High-resolution medical images; Probability distribution; High bit-depth imaging; Image quality improvement

Introduction

Magnetic Resonance Imaging (MRI) has revolutionized medical diagnostics and research by providing detailed images of internal structures without the need for ionizing radiation. The non-invasive nature of MRI, coupled with its ability to offer high-resolution images, has made it an indispensable tool in various clinical and research applications. However, the inherently slow data acquisition process remains a significant limitation. Extended scanning times can cause patient discomfort and increase the likelihood of motion artifacts, which can degrade image quality. Consequently, accelerating MRI acquisition has been a critical area of research since the inception of the technology. Initial advancements in speeding up MRI were made through the development of fast imaging sequences, such as echo planar imaging (EPI) and gradient echo sequences [1-2]. These rapid sequences significantly reduced acquisition times but introduced new challenges, such as nerve stimulation due

to the rapid switching of magnetic field gradients. This phenomenon, known as peripheral nerve stimulation, set practical limits on the acceleration achievable through these sequences. The quest for faster imaging without compromising safety and image quality led to the exploration of alternative approaches.

A transformative development in the field was the introduction of multiple receiver channels. Initially intended to improve the signal-to-noise ratio (SNR) of MRI scans, multichannel systems opened the door to parallel imaging techniques [3-5]. These techniques take advantage of the spatially distinct sensitivity profiles of multiple receiver coils to reconstruct images from undersampled k-space data. By doing so, they significantly reduce acquisition times while maintaining high image quality. Notable parallel imaging methods, such as SENSE (Sensitivity Encoding) and GRAPPA (Generalized Autocalibrating Partially Parallel Acquisitions), have since become standard in clinical MRI practice, offering substantial speed improvements.

In parallel with the development of hardware-based acceleration techniques, software-based methods like compressed sensing (CS) have also gained prominence [6-7]. CS leverages the inherent sparsity of MR images in specific transform domains, such as wavelets or total variation, to reconstruct high-quality images from undersampled data. The core idea is to solve an optimization problem that enforces both data consistency and sparsity, often requiring iterative algorithms. While these methods are computationally intensive, advances in algorithm efficiency and hardware acceleration, such as GPU-based implementations, have made CS-MRI increasingly viable for clinical use [8-10].

The emergence of deep learning (DL) has further revolutionized MRI by introducing a new paradigm for image reconstruction [11-12]. Convolutional neural networks (CNNs), a popular subset of DL, have demonstrated exceptional performance in various imaging tasks, including image classification and segmentation [11-14]. In the context of MRI, DL techniques have been applied to reconstruct images from undersampled k-space data, effectively transforming iterative reconstruction processes into direct inference tasks. This shift has enabled the development of sophisticated network architectures, such as Unet and cascaded CNNs, which mimic traditional iterative methods [14]. Despite their promise, DL-based approaches face challenges related to high memory requirements and implementation complexity, particularly when dealing with high-resolution images.

A novel and intriguing approach to MRI reconstruction involves the direct reconstruction of quantized images. Traditionally, the quantization process—where pixel intensity levels are represented using a fixed number of bits—occurs post-reconstruction, particularly in formats like DICOM. However, framing the reconstruction task as a pixel classification problem rather than a regression problem aligns well with the capabilities of DL classification networks. This approach can offer computational efficiency and enhanced noise robustness, especially in scenarios with low SNR.

This paper focuses on leveraging a deep learning framework to address image reconstruction in MRI by converting the problem into a pixel classification task. The proposed method introduces a divide-and-conquer strategy to handle high-bit precision images, specifically targeting 16-bit depth. We compare the performance of this pixel classification approach with traditional CS methods and DL regression networks, validating the framework using various datasets, including T1 and T2-weighted MR images. Furthermore, we explore the effect of noise on image reconstruction, providing a comprehensive evaluation of the proposed method's robustness and effectiveness.

Methods

To train and validate our deep learning (DL) models, we utilized T1 and T2 weighted 3D volumetric images from the publicly available IXI dataset (https://brain-development.org/ixi-dataset/). For each contrast, T1 and T2, a total of 250 subjects were employed for training, while 60 subjects were set aside for validation. The training images were created by undersampling the k-space data by a factor of 7 in two of the encoding directions, using a variable density undersampling pattern. This choice of 2D undersampling, as opposed to 1D, facilitated a higher acceleration factor of 7, reducing the likelihood of severe artifacts that might arise from the latter. For training our networks, we used the Keras deep learning library with a TensorFlow backend. The Adam optimizer, initialized with a learning rate of 0.0001, was employed, and the learning rate was decayed by a factor of 0.96 per epoch. Each epoch consisted of 2500 iterations, and the total training encompassed 150 epochs. The model corresponding to the minimum validation loss was selected as the final trained model. We compared four distinct methods for MR image reconstruction from undersampled k-space data: (i) a compressed sensing (CS) reconstruction utilizing a wavelet and total variation (TV) penalty, (ii) a DL regression reconstruction with mean squared error (MSE) loss, (iii) a DL regression reconstruction with mean absolute error (MAE) loss, and (iv) a DL classification reconstruction with 16-bit precision. These models were evaluated using three experimental setups: the IXI datasets, IXI datasets with added noise.

In the CS reconstruction approach, the parameters for wavelet and TV regularization were carefully optimized to maximize the structural similarity index (SSI). The chosen regularization parameters

were 0.0001 for wavelet and 0.0005 for TV. The reconstruction was performed using a nonlinear conjugate gradient method. For DL-based reconstructions, the final layer of the regression network predicted pixel values directly. In contrast, the classification network predicted the probability distribution for each pixel intensity, categorizing them into 256 classes. The coefficients a_0 and a_1 were computed using the network's outputs, and the final 16-bit images were obtained accordingly.

To evaluate the impact of noise, random Gaussian noise was introduced to the undersampled k-space data, resulting in Rician distributed noise in the magnitude images. The performance of each reconstruction method under these conditions was assessed, with hyperparameters for the CS method re-optimized for the noisy scenario.

Results and discussions

The deep learning classification method generates a probability distribution for each pixel, rather than assigning a direct pixel value as shown in Fig. 1. In this study, DL-C Avg reconstruction technique was utilized which uses a weighted sum of the probability distribution to approximate continuous pixel values between $[0, M-1]$, aiming to reduce quantization errors. This is expressed as:

$I(x) = \sum_{p=0}^{M-1} p \times P(p,x) (1)$

where $I(x)$ represents the reconstructed image and $P(p,x)$ is the probability distribution predicted by the DL classification network at the spatial location x for $M = 2^n$ classes, with n being the bit depth used for quantization.

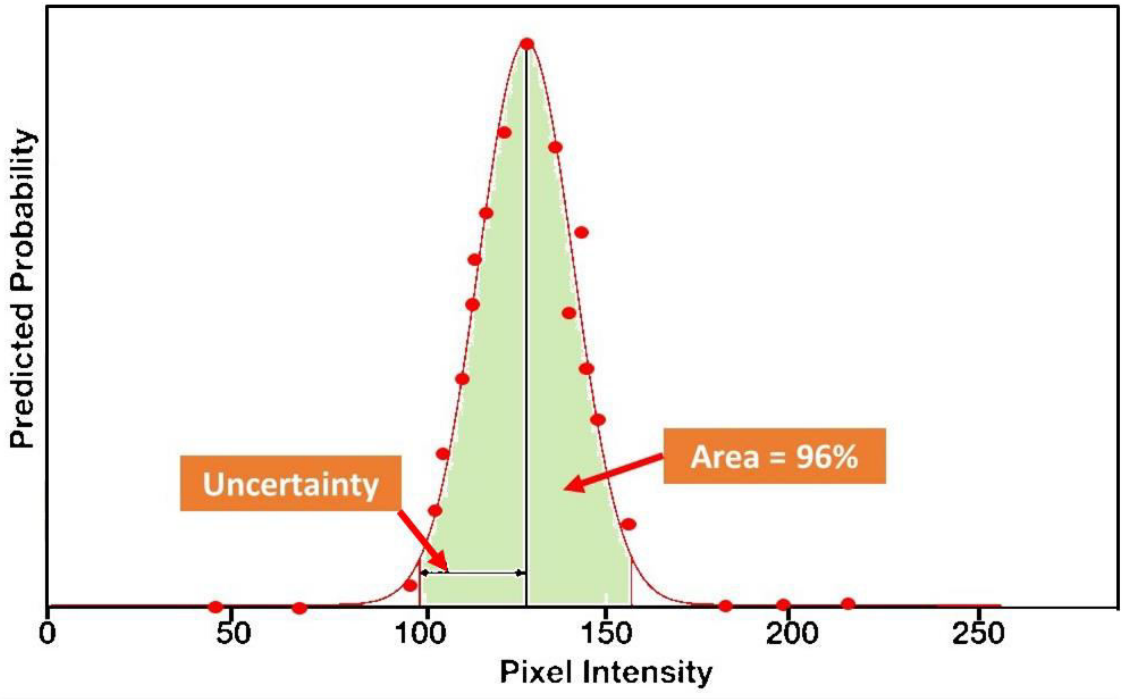

Figure 1. Probability distribution for a pixel's quantized intensities predicted by the classification network. The x-axis shows quantized pixel intensities, while the y-axis displays predicted probabilities. Uncertainty is represented by the 95% confidence interval around the mean values.

We design an encoder-decoder Unet architecture with skip connections (Fig. 2), tailored to predict the probability distribution of each pixel's intensity in the artifact-free image. The network is similar for both regression and classification tasks, except for the final layer and the loss function used. The regression network minimizes the mean absolute error between the predicted and target images, while the classification network uses softmax activation and cross-entropy loss to predict class probabilities. The network architecture's memory requirements grow exponentially with increasing bit-depth. For an n-bit unsigned integer, the dynamic range is $[0, 2^n - 1]$. To predict the probability of each pixel intensity using the proposed classification approach, 2^noutput channels are needed. This can be impractical for high bit-depth images due to the large number of required channels (65,536 channels for 16-bit depth), posing challenges in terms of physical memory and the risk of overfitting due to the sheer number of parameters. To address this, a divide-and-conquer strategy was incorporated in this study, splitting the original problem into smaller, more manageable sub-problems. These sub-problems are then solved independently, with their solutions combined to reconstruct the final high bit-depth image. The novel network architecture designed around this strategy allows for the

prediction of higher bit-depth images without a significant increase in learnable parameters. Specifically, the approach involves decomposing an n-bit integer (N) into a linear combination of two $n/2$- bit integers:

$$N = 2^{\frac{n}{2}}a_0 + a_1; \forall a_0, a_1 \in \left[0, 2^{\frac{n}{2}} - 1\right] (2)$$

The network is adapted to predict both $a_0$and $a_1$which are then used to compute N. This approach minimizes the increase in the number of parameters, making it feasible to apply the proposed method to higher bit-depth images.

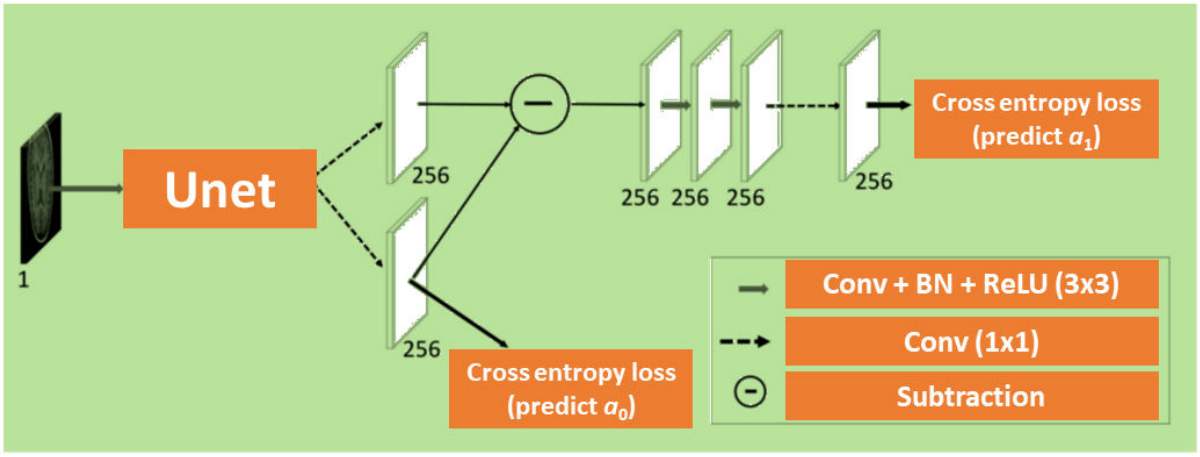

Figure 2. Network architecture for 16-bit classification, where the Unet outputs two 256-channel predictions ($a_0$and a_1) for the probability distributions of two 8-bit values. These distributions are combined to determine the final pixel value using Eq. 2.

We compared five distinct reconstruction techniques for an acceleration factor of 6. The methods include ZF (zero-filled reconstruction), where absent k-space lines are substituted with zeros and the image is reconstructed via Fourier transform; CS (compressed sensing reconstruction) utilizing total variation and wavelet regularizations; DLR-L2 (deep learning regression reconstruction) with a network trained using mean squared error; DLR-L1 (deep learning regression reconstruction) with a network optimized using mean absolute error; and DLC (deep learning classification reconstruction), which operates on 16-bit images. It is important to note that separate networks were trained for T1 and T2 weighted images. Figure 3 presents the reconstructed images for T1 and T2 weighted sequences, comparing zero-filled (ZF), compressed sensing (CS), deep learning regression with L2 loss (DLR-L2), deep learning regression with L1 loss (DLR-L1), and the deep learning classification (DLC) approaches. These reconstructions were derived based on Eqs. 1 and 2. It is evident from Fig. 3 that the compressed sensing reconstruction (CS) displays a reduction in resolution and suffers from blurred edges, as highlighted by the enlarged image sections. The DLR-L2 method also exhibited resolution loss and blurred edges, whereas the DLR-L1 reconstructions struggled to recover low-contrast features, leading to their attenuation. As shown by the black arrow in Fig. 2, the DLC reconstruction provided better delineation between white and gray matter, resulting in higher resolution and sharper edges. This was in contrast to the other methods, where low-contrast features were less distinctly recovered. The DLC network's superior performance is further supported by quantitative metrics, including the structural similarity (SSI) index, peak signal-to-noise ratio (PSNR), relative error, and mean squared error (MSE), as shown in Table 1.

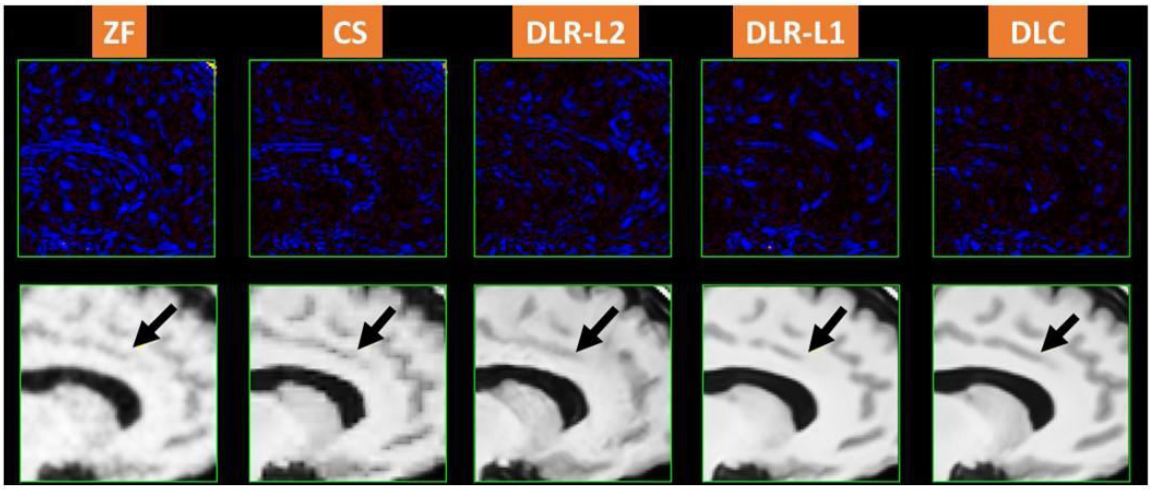

Figure 3. Comparison of T1 and T2 weighted image reconstructions using Zero-Filled (ZF), Compressed Sensing (CS), DL-Regression with L2 loss (DLR-L2), DL-Regression with L1 loss (DLR-L1), and DL-Classification (DLC) methods.

Table 1. Performance metrics for T1 and T2 weighted images.

	Structural Similarity Index (SSI)	**Peak Signal-to-Noise Ratio (PSNR)**	**Relative Error**	**Mean Squared Error (MSE)**
Quantitative Metrics for T1 weighted images				
CS	0.938	31.22	0.0498	7.924e-4
DLR-L2	0.942	32.33	0.0492	6.721e-4
DLR-L1	0.954	32.55	0.0481	6.311e-4
DLC	0.957	33.43	0.0455	6.021e-4
Quantitative Metrics for T2 weighted images				
CS	0.962	32.13	0.0522	7.122e-4
DLR-L2	0.974	33.84	0.0432	5.711e-4
DLR-L1	0.978	34.55	0.0411	4.231e-4
DLC	0.983	34.83	0.0402	4.122e-4

When working with low-field strengths, where the signal-to-noise ratio (SNR) is inherently lower, we tested the robustness of the DLC and DLR networks by introducing Gaussian noise to the dataset. This noise, complex in nature with both real and imaginary components drawn from a Gaussian distribution, was added to the undersampled k-space data, resulting in a peak SNR of approximately 18.0 dB. Figure 4 illustrates the outcomes of image reconstructions for both T1 and T2 weighted images, where Gaussian noise has been introduced. The comparison includes reconstructions using zero-filled (ZF), compressed sensing (CS), deep learning regression with L2 loss (DLR-L2), deep learning regression with L1 loss (DLR-L1), and the deep learning classification (DLC) methods, computed according to Eqs. 1 and 2. The CS method was notably impacted by the noise, leading to excessive blurring and patchy artifacts in the reconstructed images, as evident from Fig. 4. The deep learning regression networks (DLR-L2 and DLR-L1) fared better but still showed a significant loss of low-contrast features under noisy conditions. Conversely, the DLC classification network outperformed the others, delivering images with crisper edges and effectively mitigating the noise's impact. This superior performance is reflected in the quantitative scores for both T1 and T2 weighted images, as detailed in Table 2. Among these techniques, the DLC network was the most resilient to noise. Specifically, for T1-weighted images, the SSI score for the DLC method dropped by only 2.5 %, compared to declines of 3.1 %, 3 %, and 5.6 % for DLR-L1, DLR-L2, and CS, respectively.

Table 2. Performance metrics for T1 and T2 weighted images in presence of Gaussian noise.

	Structural Similarity Index (SSI)	Peak Signal-to-Noise Ratio (PSNR)	Relative Error	Mean Squared Error (MSE)
Quantitative Metrics for T1 weighted images under Gaussian noise				
CS	0.882	27.88	0.0721	1.621e-3
DLR-L2	0.912	28.09	0.0645	1.311e-3
DLR-L1	0.923	28.44	0.0632	1.291e-3
DLC	0.932	29.99	0.0611	1.124e-3
Quantitative Metrics for T2 weighted images under Gaussian noise				
CS	0.939	29.22	0.0623	1.239e-3
DLR-L2	0.962	30.98	0.0512	6.731e-4
DLR-L1	0.968	30.12	0.0542	7.931e-4
DLC	0.974	31.92	0.0482	6.222e-4

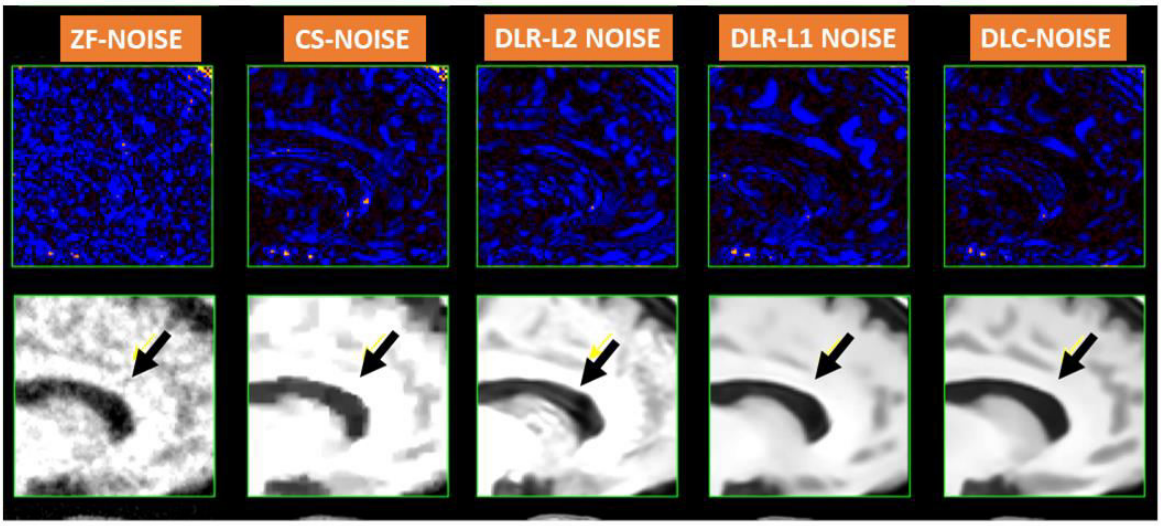

Figure 4. Reconstruction results for T1 and T2 weighted images with added Gaussian noise, comparing Zero-Filled (ZF), Compressed Sensing (CS), DL-Regression with L2 loss (DLR-L2), DL-Regression with L1 loss (DLR-L1), and DL-Classification (DLC) methods.

These results highlight the effectiveness of the deep learning classification (DLC) method for reconstructing high-resolution medical images, particularly in the presence of noise. The DLC method, which outputs a probability distribution for each pixel rather than a direct pixel value, demonstrates significant advantages over traditional reconstruction methods like zero-filled (ZF) and compressed sensing (CS), as well as deep learning regression approaches with both L1 (DLR-L1) and L2 (DLR-L2) loss functions. The comparison of the five reconstruction methods—ZF, CS, DLR-L2, DLR-L1, and DLC-L2 revealed several key insights into the performance and limitations of each technique. The ZF method, while computationally simple, results in the lowest quality reconstructions due to its inability to effectively handle missing k-space data, leading to severe aliasing artifacts. The CS method, which applies regularization techniques like total variation and wavelet transforms, improves upon ZF but still suffers from a loss of resolution and blurring of edges. This outcome is consistent with the known limitations of CS in scenarios with high acceleration factors, where the regularization may overly smooth the image, leading to the suppression of fine details. The deep learning regression methods (DLR-L2 and DLR-L1) offer a marked improvement over ZF and CS by learning the mapping from undersampled k-space to fully sampled images. However, the choice of loss function significantly impacts the quality of the reconstructed images. The DLR-L2 method, which minimizes the mean squared error, tends to blur low-contrast features and edges, likely due to the inherent bias of the L2 loss function towards minimizing large errors, which can lead to overly smooth reconstructions. On the other hand, the DLR-L1 method, which minimizes the mean absolute error, performs better in preserving edges but still struggles with low-contrast areas. This is likely because the L1 loss, while less sensitive to outliers, can still lead to artifacts in regions where subtle intensity variations are crucial. In contrast, the DLC method excels in reconstructing images with high resolution and sharp edges, as evidenced by the superior delineation of white and gray matter. The

probabilistic nature of DLC allows it to more effectively capture the full range of pixel intensities, reducing quantization errors and preserving finer image details. This is particularly important in medical imaging, where the accurate depiction of subtle tissue differences is critical for diagnosis and treatment planning. The quantitative metrics further support the superiority of DLC, with higher structural similarity (SSI) indices and peak signal-to-noise ratios (PSNR), and lower relative errors and mean squared errors (MSE). These results underscore the potential of DLC for high-quality image reconstructions, even in challenging scenarios with high acceleration factors.

The robustness of the reconstruction methods in the presence of Gaussian noise was also examined, particularly relevant for low-field strength imaging where the signal-to-noise ratio (SNR) is inherently lower. The addition of noise significantly degraded the performance of the ZF and CS methods, with CS particularly affected, resulting in excessive blurring and patch-like artifacts. The DLR methods also showed a decline in performance, with a notable loss of low-contrast features, which are critical in medical imaging for distinguishing between different tissue types. Remarkably, the DLC method maintained its high performance even under noisy conditions. The probabilistic approach of DLC, combined with its robust network architecture, allowed it to effectively filter out the noise while preserving important image features. This is evidenced by the relatively small decrease in SSI scores for DLC compared to the other methods, particularly in T1-weighted images. The DLC's ability to reconstruct sharper images with reduced noise impact suggests it is particularly well-suited for low-SNR environments, such as low-field MRI or fast imaging protocols where noise is more pronounced.

This study also addresses the challenges associated with high bit-depth imaging, which is becoming increasingly important as imaging technologies evolve to provide greater detail and dynamic range. The proposed divide-and-conquer strategy, which decomposes the problem into smaller sub-problems by splitting an n-bit number into two n/2-bit numbers, proves effective in managing the memory and computational demands of reconstructing high bit-depth images. This approach enables the DLC method to handle 16-bit images without a prohibitive increase in the number of network parameters, making it a practical solution for high-resolution medical imaging. The success of the DLC method in both high bit-depth imaging and noise robustness suggests that it could be a valuable tool for a wide range of medical imaging applications, from routine diagnostic imaging to more specialized scenarios where high image quality is paramount. The ability to accurately reconstruct images with minimal artifacts and noise, while also handling the demands of high bit-depth, positions the DLC method as a leading candidate for next-generation medical image reconstruction.

Conclusion

In summary, the deep learning classification method demonstrates clear advantages over traditional and deep learning regression methods in reconstructing high-quality medical images, particularly in challenging scenarios involving high acceleration factors, low SNR, and high bit-depths. The probabilistic nature of DLC, combined with innovative strategies to manage computational complexity, enables it to deliver superior image quality with sharp edges, preserved low-contrast features, and robustness to noise. These findings highlight the potential of DLC as a powerful tool for advancing medical imaging technologies, providing clinicians with more accurate and reliable images for diagnosis and treatment planning.

References

[1] P. Mans_eld, “Multi-planar image formation using NMR spin echoes,” *J. Phys. C, Solid State Phys.*, vol. 10, no. 3, p. 55, 1977.

[2] J. Frahm, A. Haase, and D. Matthaei, “Rapid NMR imaging of dynamic processes using the FLASH technique,” *Magn. Reson. Med.*, vol. 3, no. 2, pp. 321-327, 1986.

[3] K. P. Pruessmann, M. Weiger, M. B. Scheidegger, and P. Boesiger, “SENSE: Sensitivity encoding for fast MRI,” *Magn. Reson. Med.*, vol. 42, no. 5, pp. 952-962, 1999.

[4] D. K. Sodickson, “Tailored SMASH image reconstructions for robust *in vivo* parallel MR imaging,"*Magn. Reson. Med.*, vol. 44, no. 2, pp. 243-251, 2000.

[5] D. K. Sodickson and W. J. Manning, “Simultaneous acquisition of spatial harmonics (SMASH): Fast imaging with radiofrequency coil arrays,” *Magn. Reson. Med.*, vol. 38, pp. 591-603, 1997.

[6] M. Lustig, D. L. Donoho, J. M. Santos, and J. M. Pauly, “Compressed sensing MRI,” *IEEE Signal Process. Mag.*, vol. 25, no. 2, pp. 72-82, Mar. 2008.

[7] M. Lustig, D. Donoho, and J. M. Pauly, “Sparse MRI: The application of compressed sensing for rapid MR imaging,” *Magn. Reson. Med.*, vol. 58, no. 6, pp. 1182-1195, 2007.

[8] T. M. Quan, S. Han, H. Cho, andW. K. Jeong, “Multi-GPU reconstruction of dynamic compressed sensing MRI," in *Medical Image Computing and Computer-Assisted Intervention-MICCAI* (Lecture Notes in Computer Science), vol. 9351, N. Navab, J. Hornegger,W.Wells, and A. Frangi, Eds. Cham, Switzerland: Springer, 2015.

[9] M. Zimmermann, Z. Abbas, K. Dzieciol, and N. J. Shah, “Accelerated parameter mapping of multiple-echo gradient-echo data using model-based iterative reconstruction,"*IEEE Trans. Med. Imag*., vol. 37, no. 2, pp. 626-637, Feb. 2018.
[10] C. A. Baron, N. Dwork, J. M. Pauly, and D. G. Nishimura, “Rapid compressed sensing reconstruction of 3D non-Cartesian MRI,” *Magn. Reson. Med*., vol. 79, no. 5, pp. 2685-2692, 2018.
[11] Y. A. LeCun, Y. Bengio, and G. E. Hinton, “Deep learning,” *Nature*, vol. 521, no. 7553, pp. 436-444, 2015.
[12] G. Litjens, T. Kooi, B. E. Bejnordi, A. A. A. Setio, F. Ciompi, M. Ghafoorian, J. A. W. M. van der Laak, B. van Ginneken, and C. I. Sánchez, “A survey on deep learning in medical image analysis,” *Med. Image Anal.*, vol. 42, pp. 60-88, Dec. 2017.
[13] K. Pawar, Z. Chen, N. J. Shah, and G. Egan, “Residual encoder and convolutional decoder neural network for glioma segmentation,” *Proc. Int. MICCAI Brainlesion Workshop*, 2018, pp. 263-273.
[14] O. Ronneberger, P. Fischer, and T. Brox, “U-Net: Convolutional networks for biomedical image segmentation," in *Proc. MICCAI*, 2015, pp. 234-241.